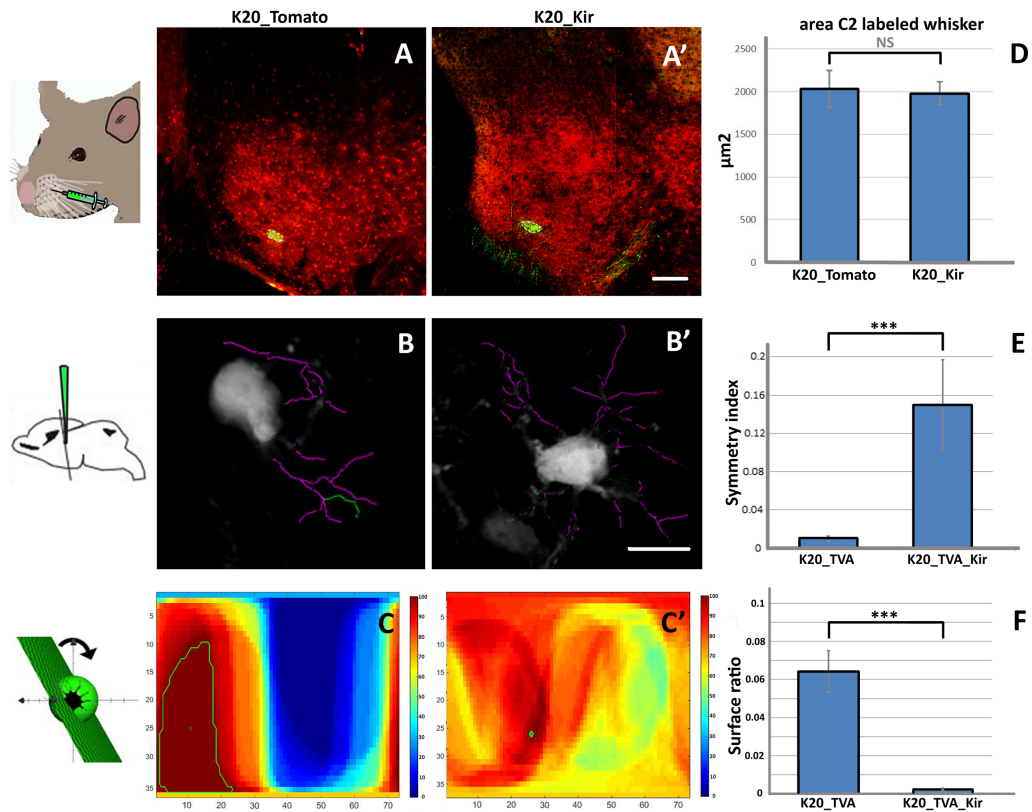
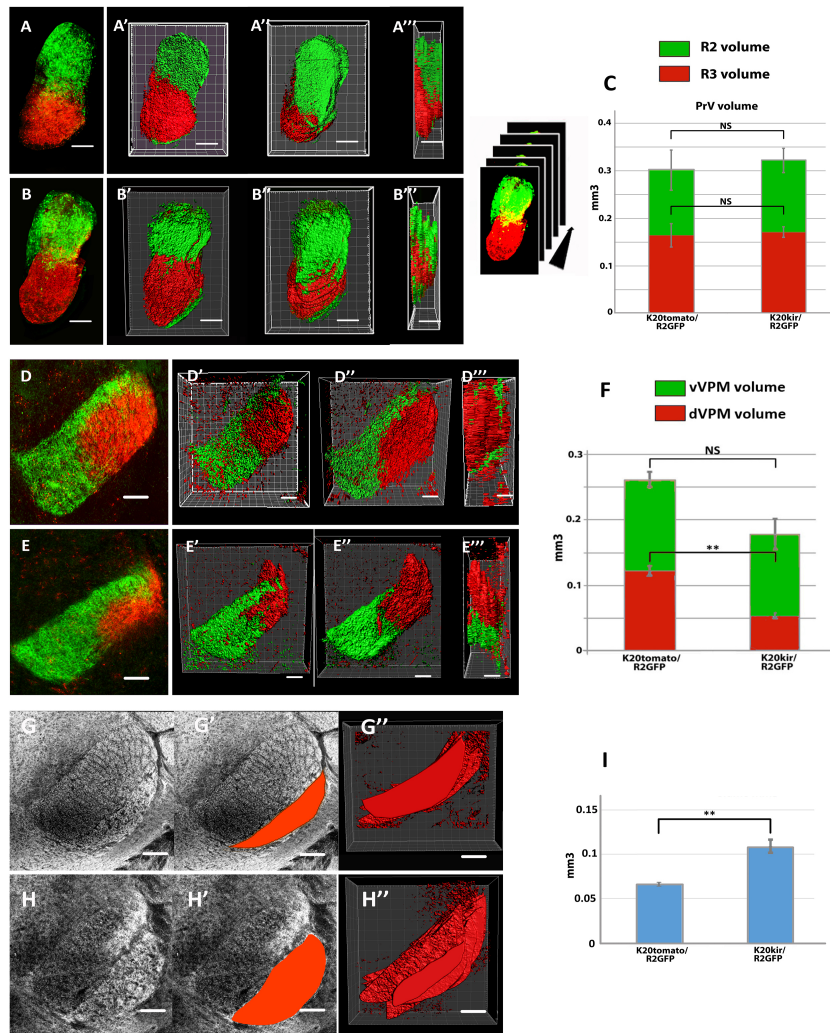


**Figure 1.** Prenatal overexpression of Kir2.1 in the ventral PrV alters the correct formation of the Barrelettes-Barreloids-Barrels map. (A-C) CO oxidase staining performed at P8 in wt and K20\_Kir mice show the absence of the barrelette pattern in the brainstem (A and A') of the mutant animals despite a same PrV area (A''). Although highly perturbed and shrunk (B'' and C''), the Barreloids and Barrels patterns are still present in the thalamus and cortex, respectively (B' and C'). Vglut2 staining of coronal sections confirms the shrinkage of the barreloids (D,D') and barrels areas (E,E') despite the presence of a residual patterning (E' high magnification). Scale bars 200  $\mu$ m.



**Figure 2.** Prenatally perturbation of neuronal activity in the ventral PrV perturbs the dendrite orientation of barrelette neurons without altering the patterning of the trigeminal ganglion neuron afferents. Dextran labelling of trigeminal axons from a single whisker (C2) at P4 shows no difference of axonal patterning and organization among wt and K20\_kir mice (A and D). Dendrite orientation of barrelette neurons at P10, observed upon expression of pseudotyped rabies virus (EnvA-SADΔG-GFP) after thalamic injection at P3 in K20\_TVA and K20\_TVA\_Kir mice, shows the absence of an asymmetric dendritic arbor orientation in mutant animals (B). Different Symmetric index (E) and surface ratio (F) in wt and mutant animals, calculated upon Matlab® analysis, show a significant absence of asymmetric tree orientation of neuronal barrelettees in K20\_Kir mice. Analysis was done upon a dividing the neuronal dendritic arbor in two half spheres and calculating the ratio among the dendritic densities. Example of the 2592 ratios calculated for a wt (C) and K20\_kir (C') barrelette neurons are shown using a colour code. T-test two tails in E and F (n=3 wt and mut.),  $P < 0.001$ . Scale bars: 200 µm in A and A'; 10 µm B and B'.



**Figure 3.** Prenatal perturbation of neuronal activity in the ventral PrV impairs the volume of somatosensory thalamic target nuclei without affecting the size of brainstem nuclei. 2.5-D multislice reconstructions of the PrV in the wt (k20\_tomato/Rhombomer2\_GFP -R2GFP-) and mutant (K20\_kir/R2GFP) animals show that the sizes of the ventral and dorsal PrV are not affected at P8 upon expression of the Kir2.1 in the ventral PrV at prenatal stage (A-C). 2.5-D multislice reconstructions of thalamic VPM at P8 show that the volume of the R3 targeted area in the dorsal VPM (red labelled) is smaller in the K20-kir mice when compared with the wt animals; on the contrary, the volume of the R2 targeted area is not affected upon Kir2.1 in the ventral PrV at prenatal stage (D-F). 2.5-D multislice reconstructions of thalamic VPM stained against Vglut-2 antibody show a significant expansion of the VPL nuclei in the K20\_kir mice at P8 (G-I). 2.5-D multislice reconstructions were made using Fiji® and Imaris®. T-Test 2 tails in C, F and I ( $n \geq 3$  for wt and mut.);  $P < 0.01$  in F and I, NS= not significant. Scale bars: 200  $\mu\text{m}$ .

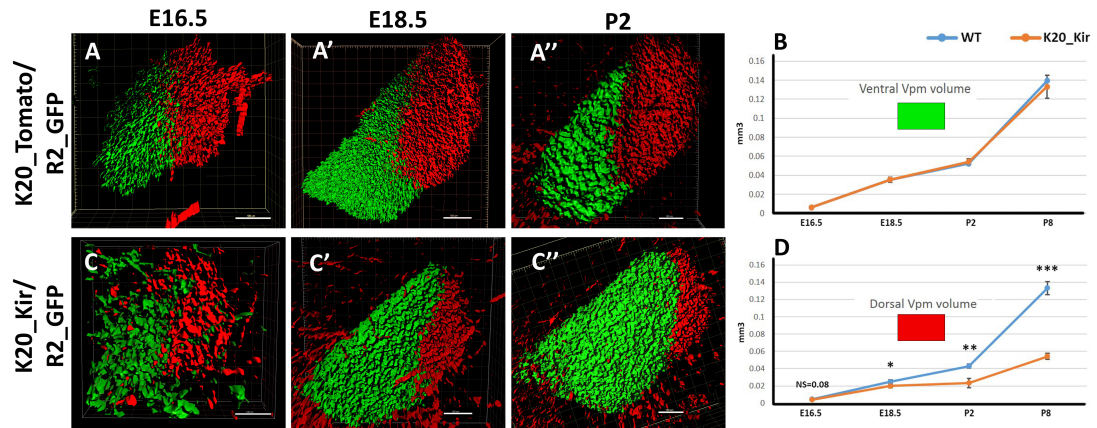


**Figure 4. Volume of the VPM thalamic nuclei analysed through a time-course at different stages of development.** 2.5-D multislice reconstructions of thalamic VPM at E16.5 (A,C), E18.5 (A', C') and P2 (A'' and C'') in wt (K20\_Tomato/R2GFP) and mutant (K20\_Kir/R2GFP) animals. Time course analysis shows that the volume of the ventral VPM, which is targeted by GFP labelled neurons located in the dorsal PrV, is not affected during pre- and post-natal development upon early perturbation of the neuronal activity in the ventral PrV (B). On the contrary, time course analysis shows that the volume of the dorsal VPM, which is targeted by red-labelled neurons located in the ventral PrV (TdTomato and mcherry within wt and mutant animals, respectively), is already smaller at prenatal stages in K20\_Kir mice (D). 2.5-D multislice reconstructions were made using Fiji® and Imaris®. T-Test 2 tails using a Bonferroni correction in B and D (n=3 for wt and mut for each stage); P<0.05, <0.01 and <0.001 using one, two or three asterisks, respectively. Scale bars= 100 µm.

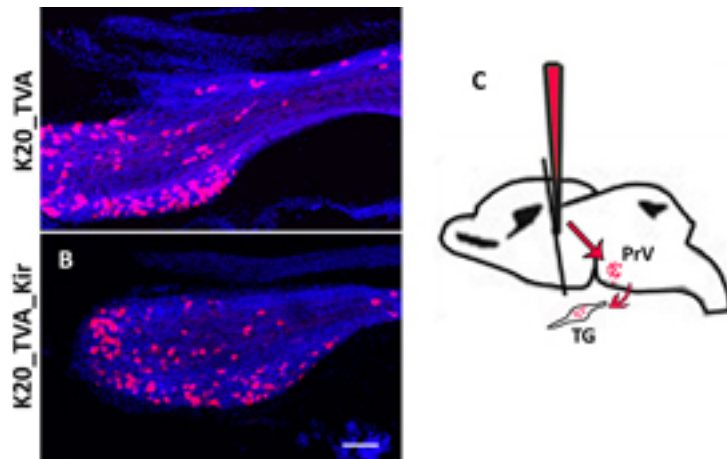


**Fig. 5. Neurons in the PrV are still monosynaptically connected with Trigeminal Ganglion neurons upon prenatal perturbation of the neuronal activity.** Labelled trigeminal ganglion neurons at P10 upon VPM injections at P3 of EnvA-SADΔG-mcherry and Herpes Simplex Virus 1-Glycoprotein (HSV1-G) in wild type (K20\_TVA) and mutant (K20\_TVA\_Kir) mice (A,B). Schematic shows how the EnvA-pseudotyped rabies virus, once complemented with a Glycoprotein provided by an HSV-virus, is able to jump monosynaptically from the PrV to the trigeminal ganglion (C). Scale bar 200  $\mu$ m.